Single-electron tunneling in a single PbS nanocrystal nucleated on 11-mercaptoundecanoic acid self-assembled monolayer at room temperature

Peng Jiang[a)]
Beijing Laboratory of Vacuum Physics, Institute of Physics & Center for Condensed Matter Physics,
Chinese Academy of Sciences, P.O. Box 2724, Beijing 100080, People's Republic of China

Zhong-Fan Liu and Sheng-Min Cai
Center for Nanoscale Science & Technology (CNST) and College of Chemistry and Molecular Engineering,
Peking University, Beijing 100871, People's Republic of China

Nanometer-sized PbS particles in the size of about 3 nm produced by exposing a self-assembled monolayer of 11-mercaptoundecanoic acid salts on gold (111) substrate in a H_2S atmosphere were studied by scanning tunneling microscopy (STM) and high-resolution transmission electron microscopy at room temperature in air. The stability of thus-obtained PbS nanoparticles makes STM imaging possible and repeatable scans of the semiconductor nanoparticles were performed. The current-voltage ($I–V$) characteristics of a single PbS nanoparticle exhibited clearly Coulomb blockade and Coulomb staircase. Furthermore, by varying the gap between a STM tip and the PbS nanoparticle, we also verified the dependence of staircase width on the change of the gap in the local $I–V$ characteristics on the same PbS nanoparticle. The phenomena can be well described by a semi-classical double-barrier tunneling model. © *2001 American Institute of Physics.*
[DOI: 10.1063/1.1382827]

Single-electron tunneling (SET) phenomena have attracted long-standing interest due to their potential application in future single-electron devices.[1–3] The phenomena have been investigated in many nanostructures, in which a small metal or semiconductor island, the so-called "Coulomb island," is coupled to an external circuit through two tunnel junctions.[4,5] In order to observe the SET behavior at room temperature, the size of the center island should usually be reduced down to be less than 10 nm to meet the requirement that the charging energy of a quantum dot must exceed the thermal energy ($e^2/C > kT \approx 26$ meV). Ordered organic monolayers have proven to be versatile as templates for the formation of smaller inorganic nanocrystals with a high degree of monodispersity. Up to now, various semiconductor nanoparticles have been synthesized by employing the methodology. However, most of the studies used Langmuir–Blodgett (LB) monolayers[6] or multilayer self-assembly films[7] as templates, and only a few reports[8] were focused on directly nucleating semiconductor nanoparticles on only one layer of organic self-assembled monolayer. In this communication, we describe a strategy for growing PbS nanoparticles on the Au (111) substrates modified by 11-mercaptoundecanoic acid self-assembled monolayer (SAM). Then, a single thus-obtained PbS nanoparticle was directly used to construct a double-barrier tunneling junction (DBTJ) system with a scanning tunneling microscopy (STM) tip.

The preparation method has been described previously.[8] In this experiment, lead ions (Pb^{2+}) in $Pb(NO_3)_2$ solution were selected as adsorbed cations. A typical STM image of the PbS nanoparticles formed on a Au (111) surface through the SAM coupling layer is shown in Fig. 1(a). It is seen that almost all of the PbS nanoparticles are oriented roughly in the same direction, which probably implies the long-range order of the SAM on Au (111). The apparent mean diameter of the PbS nanoparticles was measured by section analysis from 100 the PbS nanoparticles as shown in Fig. 1(a) to be 3.2 ± 0.4 nm. To further verify the formation of the PbS nanoparticles, we also synthesized PbS nanoparticles on STM gold-tip apex using the similar method. Thus-modified Au tips can be directly used for TEM observation. Figure 1(b) demonstrates a TEM image of the apex region of the SAM/PbS-modified gold tip, on which a single ~4 nm sized PbS nanoparticle was clearly observed. The lattice constant between the planes was found to be 0.34 nm, very consistent with that of PbS{111}($d = 0.3429$ nm).

The $I–V$ characteristics of a single PbS nanoparticle were detected with the STS mode by locating a chemically etched gold STM tip over a chosen PbS nanoparticle about 3 nm in size. Due to the long-term scanning stability of the sample, it is possible to measure a series of $I–V$ characteristics with the respect to the z displacement of the tip. In Fig. 2, we display such $I–V$ curves as a function of the tunnel current setpoint, in which clear Coulomb blockade and staircases are found. For clarity, the corresponding dI/dV curves were also plotted in Fig. 2, which show a series of equidistant peaks. The average distance between two adjacent peaks was found to be dependent on the setpoint current, varying from 240 to 160 mV with the setpoint current from 1 to 4 nA. Corresponding electrostatic charging energy of the system is in a range of 120 to 80 meV, which is much higher than the thermal excitation energy at room temperature (~26 meV). The voltage steps allow us to estimate the tunneling capacitance C_Σ, which was found to be from ~6.7 $\times 10^{-19}$ F to ~1.0×10^{-18} F with the setpoint variation.

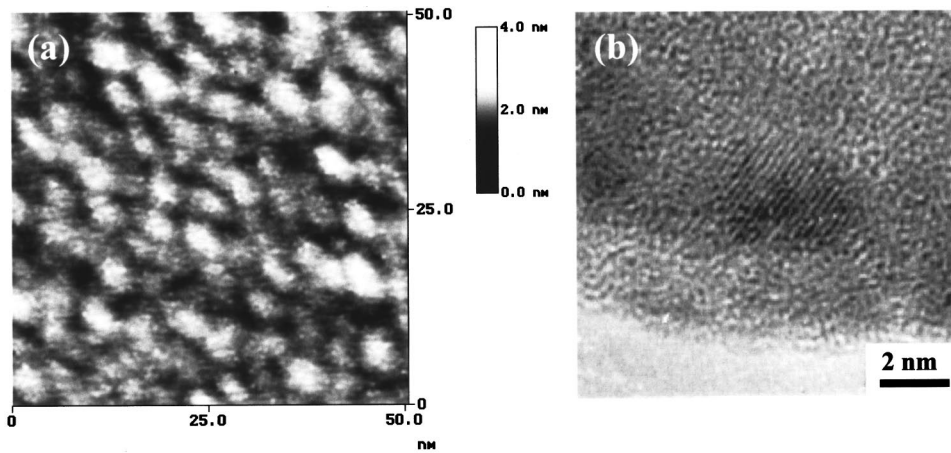[a)]Author to whom correspondence should be addressed. Electron mail: pjiang@aphy.iphy.ac.cn

FIG. 1. (a) STM image of PbS nanoparticles formed on Au (111) surface and (b) high-resolution TEM image of one PbS nanoparticle on Au tip apex.

Each is in the same order $(C = \sim 2.9 \times 10^{-18}\,\mathrm{F}$, $C = 4\pi r \varepsilon_0 \varepsilon_r$, $\varepsilon_{r(\mathrm{PbS})} = 17.9)$ as estimated from simple calculation based on a spherical 3.0 nm sized PbS nanoparticle. In addition, asymmetric shapes in positive and negative bias voltage areas were also observed in the $I{-}V$ curves, suggesting that a nonzero fraction charge Q_0 might exist on the PbS nanoparticle. The occurrence of some wider peaks in the $dI/dV{-}V$ dependences might indicate the existence of additional substructure smeared by higher temperature.

It is worth noting that similar phenomena have also been observed in our previous work, in which a CdS nanoparticle was tethered on a STM tip for SET measurements.[8] Compared with the present one, we found that each Coulomb stepwidth of voltage at a given setpoint in a PbS system was smaller than that in a CdS system, showing that the total capacitance (C_Σ) at each setpoint in the former is much larger than that in the latter. Further analysis of the STM and TEM images of both systems revealed a bigger PbS nanoparticle in size, which might be an origin of the difference. Furthermore, the geometry difference between the nanoparticle at the tip for CdS and that on the substrate for PbS might contribute to the complicated behaviors. It is unclear whether the material factor can have an additional contribution. In-depth research is needed before the root can be distinctly elucidated.
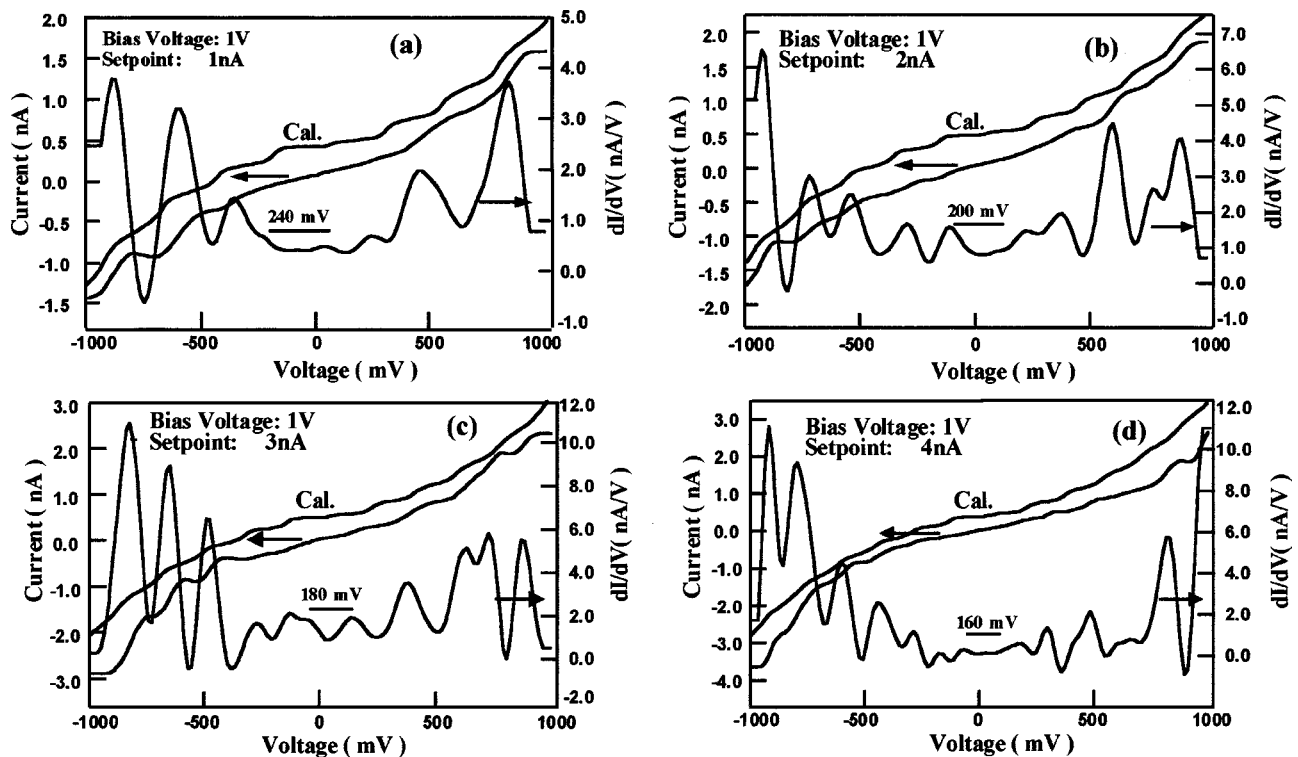

FIG. 2. The Coulomb staircases observed at various setpoint tunneling currents on a selected PbS nanoparticle. The fitting curves (thin solid lines) are obtained by the global best fitting in terms of semi-classical tunneling theory. The junction parameters for various setpoint currents are (a) $C_1 = 6.7 \times 10^{-19}\,\mathrm{F}$, $C_2 = 2.9 \times 10^{-19}\,\mathrm{F}$, $R_1 = 1200\,\mathrm{M\Omega}$, $R_2 = 21\,\mathrm{M\Omega}$, $Q_0 = -0.3e$, $\alpha = 1$. (b) $C_1 = 8.0 \times 10^{-19}\,\mathrm{F}$, $C_2 = 2.9 \times 10^{-19}\,\mathrm{F}$, $R_1 = 1020\,\mathrm{M\Omega}$, $R_2 = 21\,\mathrm{M\Omega}$, $Q_0 = 0$, $\alpha = 1$. (c) $C_1 = 8.9 \times 10^{-19}\,\mathrm{F}$, $C_2 = 2.9 \times 10^{-19}\,\mathrm{F}$, $R_1 = 600\,\mathrm{M\Omega}$, $R_2 = 21\,\mathrm{M\Omega}$, $Q_0 = 0.3e$, $\alpha = 1$. (d) $C_1 = 1.0 \times 10^{-18}\,\mathrm{F}$, $C_2 = 2.9 \times 10^{-19}\,\mathrm{F}$, $R_1 = 470\,\mathrm{M\Omega}$, $R_2 = 21\,\mathrm{M\Omega}$, $Q_0 = 0$, $\alpha = 1$, and $T = 298\,\mathrm{K}$.
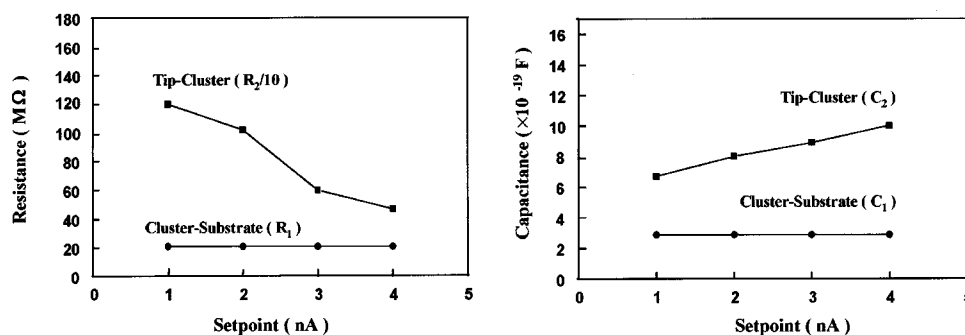
FIG. 3. Plot of fitting parameters as a function of setpoint of current employed for the I-V curves shown in Fig. 3.

By considering the structure as a DBTJ system, we can assume that the first junction is the air gap between the gold tip and the PbS nanoparticle, and the second is the 11-mercaptoundecanoic acid monolayer between the PbS nanoparticle and the Au (111) substrate. Each junction has a capacitance, an effective resistance, and a tunneling rate associated with it, denoted by C_i, R_i, and Γ_i, $i=1$, 2. In such a DBTJ model, we find that varying the locked tunnel current setpoint is in fact to change the asymmetry of the structure, in which the second barrier is rigidly fixed, whereas the air junction can be adjusted by changing the vertical distance between the nanoparticle and the tip. Therefore, moving the tip towards the PbS island can make C_1 increase so that results in the decrease of the Coulomb blockade ($\Delta V = e/C_\Sigma$) width and the increase of the corresponding staircase number.

Based on the previous discussion, a computer simulation was performed in terms of a semi-classical DBTJ model.[9–11] In order to reflect the nonlinear background and asymmetric nature in the I–V curves, we set a bias dependent resistance $R(V) = R_0/(1 + \alpha V^2)$ (Ref. 12) into the general tunneling rate Γ at the double tunneling junctions and a fractional charge Q_0 in fitting procedure. As the partial derivatives of $I(T,V; C_1, C_2, R_1, R_2, Q_0)$ cannot be represented analytically, a best fit was obtained by allowing the capacitances and resistances to be varied to find a global minimum in the mean square deviation of a theoretical $I(V)$ calculation from experimental results. Of course, reaching the global best fit was time consuming. In the process, we limited the searching region in the range of overall slope of $I(V)$ curve. A coarse search over a wide range of the variables was performed before the fine search. The average stepwidth of voltages was used to determine C_Σ. It can be seen from Fig. 2 that the experimental Coulomb staircase I–V curves are fitted well. However, some significant differences still exist in the distances of the steps between the calculated and the measured curves, which may have resulted from ignoring the quantum size effect of the isolated PbS nanoparticle in the fitting process. The tunneling resistance R_i and capacitance C_i obtained from the theoretical calculation are plotted as a function of the setpoint current in Fig. 3. The comparison can help us to judge if junction parameters would vary sensitively with the shift of the tip down to the PbS nanoparticle.

As shown in Fig. 3, it appears that a rapid decrease in R_1 and a slightly increase in C_1 are found as the gap between the tip and the PbS nanoparticle decreases, while the resistance R_2 and capacitance C_2 between the PbS nanoparticle and the Au substrate remain constant at the same time. The R_1C_1/R_2C_2 values calculated from the fitting parameters fall in a range between 77 and 132, suggesting the highly asymmetric property of the two tunnel junctions, which can be believed to be the origin of Coulomb staircases.

In summary, an ultra-small DBTJ system has been established by combining self-assembly, in $situ$ chemical reaction, and STM techniques, in which a single PbS semiconductor nanoparticle is employed as a center Coulomb island. When placing a STM tip over the nanoparticle for local I–V measurements, the clear Coulomb blockade and staircases have been observed at room temperature in air. Moreover, we have also found the vertical position dependent I–V characteristics in the electrical measurements of the chosen PbS nanoparticle, which can be attributed to the systematic variation of junction parameters. The phenomena can be well described by a semi-classical DBTJ theory. The study on I–V dependence of a PbS nanoparticle on the horizontal position will be our next target. Anyway, this work may be of value in fabricating nanoelectronic devices by direct in $situ$ chemical reaction method.

[1] H. Grabert and M. H. Devoret, Eds., *Single-Charge Tunneling, Coulomb Blockade Phenomena in Nanostructure* (Plenum, New York, 1992).
[2] D. K. Ferry, H. L. Grubin, C. Jacoboni, A. P. Jauho, *Quantum Transport in Ultrasmall Devices* (Plenum, New York, 1994).
[3] M. A. Kastner, Nature (London) **389**, 667 (1997).
[4] P. R. Andres *et al.*, Science **272**, 1323 (1996).
[5] D. L. Klein, R. Roth, A. K. L. Lim, A. P. Alivisatos, and P. L. McEuen, Nature (London) **389**, 699 (1997).
[6] W. Shenton, D. Pum, U. B. Sleytr, and S. Mann, Nature (London) **389**, 585 (1997).
[7] H. Bekele, J. H. Fendler, and J. W. Kelly, J. Am. Chem. Soc. **121**, 7266 (1999).
[8] P. Jiang, Z. F. Liu, and S. M. Cai, Appl. Phys. Lett. **75**, 3023 (1999).
[9] E. Hanna and M. Tinkham, Phys. Rev. B **44**, 5919 (1991).
[10] M. Amman, R. Wilkins, E. Ben-Jacob, P. D. Maker, and R. C. Jaklevic, Phys. Rev. B **43**, 1146 (1991).
[11] K. Mullen, E. Ben-Jacob, R. C. Jaklevic, and Z. Schuss, Phys. Rev. B **37**, 98 (1998).
[12] K. H. Park, J. S. Ha, W. S. Yun, M. Shin, K. W. Park, and E. H. Lee, Appl. Phys. Lett. **71**, 1469 (1997).